MOLECULAR AND CELLULAR BIOLOGY, Nov. 1991, p. 5592–5602
0270-7306/91/115592-11$02.00/0
Copyright © 1991, American Society for Microbiology
Vol. 11, No. 11

The *CDC20* Gene Product of *Saccharomyces cerevisiae*, a β-Transducin Homolog, Is Required for a Subset of Microtubule-Dependent Cellular Processes

NEERJA SETHI,[1] M. CRISTINA MONTEAGUDO,[1] DOUGLAS KOSHLAND,[2] EILEEN HOGAN,[2] AND DANIEL J. BURKE[1]*

Department of Biology, Gilmer Hall, University of Virginia, Charlottesville, Virginia 22901,[1] and Department of Embryology, Carnegie Institution of Washington, Baltimore, Maryland 21211[2]

Received 11 June 1991/Accepted 19 August 1991

Previous analysis of *cdc20* mutants of the yeast *Saccharomyces cerevisiae* suggests that the *CDC20* gene product (Cdc20p) is required for two microtubule-dependent processes, nuclear movements prior to anaphase and chromosome separation. Here we report that *cdc20* mutants are defective for a third microtubule-mediated event, nuclear fusion during mating of G_1 cells, but appear normal for a fourth microtubule-dependent process, nuclear migration after DNA replication. Therefore, Cdc20p is required for a subset of microtubule-dependent processes and functions at multiple stages in the life cycle. Consistent with this interpretation, we find that *cdc20* cells arrested by α-factor or at the restrictive temperature accumulate anomalous microtubule structures, as detected by indirect immunofluorescence. The anomalous microtubule staining patterns are due to *cdc20* because intragenic revertants that revert the temperature sensitivity have normal microtubule morphologies. *cdc20* mutants have a sevenfold increase in the intensity of antitubulin fluorescence in intranuclear spindles compared with spindles from wild-type cells, yet the total amount of tubulin is indistinguishable by Western immunoblot analysis. This result suggests that Cdc20p modulates microtubule structure in wild-type cells either by promoting microtubule disassembly or by altering the surface of the microtubules. Finally, we cloned and sequenced *CDC20* and show that it encodes a member of a family of proteins that share homology to the β subunit of transducin.

Microtubules are ubiquitous structures in most eucaryotic cells and are important for motility and cell structure. Microtubules are composed primarily of α- and β-tubulin heterodimers and a number of less abundant microtubule-associated proteins (13, 45). Identifying proteins that are structural components of microtubules as well as the accessory proteins that modulate microtubule assembly and function is a prerequisite to understanding the complex properties of microtubules. For example, during in vitro assembly microtubules exhibit an extraordinary behavior termed dynamic instability, alternating between stages of elongation and shortening (41). Dynamic instability has been implicated in explaining how microtubules accomplish a variety of intracellular morphogenetic events (35, 36). Microtubule assembly in vivo also displays dynamic instability (55, 59), and one important goal in research on microtubule function is to identify the proteins or other intracellular regulatory molecules that govern the dynamics of microtubule assembly.

The yeast *Saccharomyces cerevisiae* provides an attractive system with which to study several aspects of microtubule function. There are simple microtubule structures in yeast cells (6, 48) that participate in a small number of processes that involve movements of nuclei or chromosomes. Karyogamy, the process of nuclear fusion during mating of G_1 cells, is mediated by cytoplasmic microtubules (6, 7, 8, 12, 28). After DNA synthesis, the nucleus migrates, in a microtubule-dependent manner, to the neck between the mother and daughter cell prior to mitosis (6, 28, 31). Nuclear transits are microtubule-dependent oscillations of chromosomes within the nucleus that occur just prior to anaphase (47). Finally, mitotic and meiotic chromosome segregation is mediated by the microtubules in the spindle (6, 23, 28). The microtubule-dependent events are easily monitored, can be quantified, and are temporally distinct (8, 14, 23, 47).

The ease of both classical and molecular genetic analysis in *S. cerevisiae* has provided an excellent opportunity to begin a genetic dissection of microtubule assembly and function (27). There are simple, sensitive genetic assays for chromosome segregation (23, 37, 65, 66) and karyogamy (9, 14) that have been used as a basis for isolating mutants that affect microtubule-mediated processes (9, 26, 66). In addition, benzimidazole drugs that eliminate microtubule function have been used to identify mutants with altered resistance (68, 69). Several mutants have been identified that define genes encoding important structural components of microtubules such as the α-tubulin genes, *TUB1* and *TUB3*, and β-tubulin gene, *TUB2*, as well as a molecular motor of the kinesin family encoded by *KAR3* (40, 43, 57, 58, 67, 69). Both the *TUB1* gene, which produces approximately 90% of the α-tubulin, and the *TUB2* gene, which produces all of the β-tubulin, are essential for cell viability. All microtubule-mediated events are affected in temperature-sensitive *tub1* and *tub2* mutants, and cells grown at the restrictive temperature accumulate at G_2/M in the cell division cycle and therefore have a *cdc* phenotype (28, 58). *KAR1* is also an essential *cdc* gene that affects microtubule function (51). These observations show that mutants lacking proteins required for microtubule assembly and function will be pleiotropic, affecting a variety of microtubule-dependent processes, and will arrest in cell division with a *cdc* phenotype. There are other genes required for optimal microtubule function that are nonessential (mutants are viable), suggest-

* Corresponding author.

ing that they are accessory proteins that enhance the function of microtubules. One intriguing example, the *CIN4* gene, has been cloned and sequenced, and the deduced protein sequence has homology with the α-subunit of mammalian transducin (3). *CIN4* could play a role in intracellular signalling events required for regulating microtubule assembly.

cdc20 mutants were originally described by Hartwell and colleagues as causing cells to arrest after DNA synthesis in the G_2 stage of the cell cycle (22). Greater than 90% of the cells in strains with the *cdc20-1* mutation arrest at the restrictive temperature as large budded cells with a single nucleus positioned in the neck between the mother and daughter cell (50). Ultrastructural analysis of *cdc20* mutants has shown that the cells contain a short spindle, suggesting that the mutants arrest prior to anaphase (7). *cdc20* mutants show a 100-fold-higher rate of chromosome loss than do wild-type cells after growth at the semipermissive temperature, suggesting that when cells are limited for *CDC20* function, the accuracy of chromosome segregation, and mitotic spindle function in particular, is impaired (23). Finally, *cdc20* mutants are defective for nuclear movements prior to anaphase (nuclear transits), which suggests a function for *CDC20* in a second microtubule-mediated event (47). Therefore, *cdc20* mutants are similar to *tub* mutants in causing cells to arrest cell division in G_2/M prior to anaphase and in affecting more than one microtubule-mediated event.

We reasoned that *CDC20* may encode a protein that is either an essential structural component of microtubules or a regulator of microtubule assembly. In this report, we characterize further the phenotype of *cdc20* mutants and show, by indirect immunofluorescence, that microtubule structures are affected. We show that *cdc20* mutations affect karyogamy, but not nuclear migration during the mitotic cycle. Finally, we report on isolating the gene by molecular cloning and show that the predicted protein product has homology with the β subunit of mammalian transducin.

MATERIALS AND METHODS

Strains and media. Genotypes and sources of the strains used in this study are listed in Table 1. All strains except XS144-S-19 and XS144-S-22 are congenic with strain A364A (21), and all alleles were originally from Lee Hartwell's collection. Strains were constructed by standard genetic methods (64). Isogenic petite strains were isolated after growth in ethidium bromide (10 μg/ml) (64). Strains that were unable to use glycerol as a carbon source were isolated, and petite [*rho*^{0}] strains lacking mitochondrial DNA were identified as those lacking extranuclear staining with 4',6-diamidino-2-phenylindole (DAPI) (0.5 μg/ml; Sigma Chemical Co.) (74).

Yeast media YM-1, YEPD, YEPG, and SC were as described previously (21, 64). Cycloheximide was added to the YEPD medium at a final concentration of 10 μg/ml. Nocodazole (Sigma) was added from a 3.3-mg/ml stock in dimethyl sulfoxide to a final concentration of 15 μg/ml (31). Bacteria were grown in L broth (54), and plasmids were maintained by growth in selective medium with ampicillin (50 μg/ml) or kanamycin (40 μg/ml) added to the L broth or 2% LB agar.

Genetic techniques and transformation. Yeast mating, sporulation, and tetrad analysis were performed as described previously (64). Yeast transformations were performed by the lithium acetate method (30). Transformants were plated on SC medium lacking either leucine or uracil to select for the plasmid.

TABLE 1. Strains and plasmids

Strains or plasmid	Genotype	Source
Strains		
H20C1A1	*MATa his7 ura1 cdc20-1*	L. Hartwell
405-1-1	*MATa his3 ura3 ade2 cdc20-1*	Burke lab
406-2-1	*MATa his3 ura3 ade5 leu2 cdc20-1*	Burke lab
700-3-3	*MATa his7 ura1*	Burke lab
440-1-1	*MATa bar1 his7 cdc20-1*	Burke lab
4958-8-3	*MATα bar1 ade2*	Burke lab
4958-3-2	*MATa bar1 his6*	Burke lab
404-4-1	*MATα his3 ura3 hom3 cyh2 can1 cdc20-1*	Burke lab
404-4-12	*MATα his ura3 hom3 cyh2 can1 cdc20-1* [*rho*^{0}]	Burke lab
BS213	*MATa kar1-1 ura3 leu2 his7*	B. Scalafani
5100-3-2	*MATα his7 leu1 trp5 cyh2 lys5 ade5 ade2 cyh2* [*rho*^{0}]	L. Hartwell
5503-9-2	*MATa ade1 arg4 aro2 his7 lys5 met4 ura2*	L. Hartwell
GN46	*MATα kar1-1 leu2 ura3 lys2*	Koshland lab
DK5201-4-3	*MATa cdc20-1 leu2 ade2 ade3 cyh2 can1*	Koshland lab
XS144-S-19	*MATa met13 leu1 trp5 cyh2 aro2 lys5 ade5*	YGSC[a]
XS144-S-22	*MATα met13 leu1 trp5 cyh2 aro2 lys5 ade5 gal1 gal2*	YGSC
tsm 137	*MATa ade1 ade2 tyr1 lys2 his7 ura1 gal1 tsm137*	YGSC
461	*Mata/Matα ade2/ade2 his3/his3 ura3/ura3 lys5/+ cyh2/+ trp1/+ leu2/+ cdc20/+*	Burke lab
Plasmids		
pDK362	*CDC20 ARS1 CEN4 LEU2* plasmid with 17 kb of genomic DNA	
pMCM28	*CDC20 ARS1 CEN4 LEU2* plasmid that contains 2.0-kb *Hin*dIII fragment from pDK362	
pMCM23	*Eco*RI-*Hin*dIII fragment from *CDC20* in YIp352; for gene disruption	
pMCT1	pDK362 with Tn*5* insertion	
pMCT2	pDK362 with Tn*5* insertion	
pMCT10	pDK362 with Tn*5* insertion	
pMCT14	pDK362 with Tn*5* insertion	
pMCT15	pDK362 with Tn*5* insertion	

[a] YSGC, Yeast Genetics Stock Center.

Immunofluorescence. Yeast strains 405-1-1 (*cdc20*) and 700-3-3 (*CDC20*) were grown in YM-1 medium at 23°C to a cell density of 1×10^6 to 5×10^6 cells per ml. The cultures were shifted to the restrictive temperature (36°C) for 4 h and then prepared for immunofluorescence by the method described by Kilmartin and Adams (34). α-Factor-arrested cells were prepared for immunofluorescence as follows. Strains 440-1-1 (*MATa bar1 cdc20*) and 4958-3-2 (*MATa bar1 CDC20*) were grown to 10^5 cells per ml at 23°C in YM-1 medium. Synthetic α-factor (Sigma) was added to a final concentration of 0.15 μM at 23°C for sufficient time to obtain 70% of the cell population as unbudded cells. Cultures were shifted to the restrictive temperature (36°C) for 4 h, and the cells were stained with antitubulin antibody YOL 1/34 (Bioproducts for Sciences Inc.) as described above. Cells were viewed with a Zeiss Axiophot microscope equipped with

epifluorescence and photographed with Kodak T-Max 400 film. The films were developed for 7 min with T-Max developer (Kodak) at room temperature as instructed by the manufacturer.

Intranuclear tubulin immunofluorescence was quantified by using a Dage silicon-intensified target camera and a Gould digitizing image processor at the Image Processing Center, University of Virginia. The camera was calibrated with commercial standards, and all measurements were within the linear range of the camera. Images were displayed on a video screen, the area was determined, and the pixel density was measured. The total fluorescence within the intranuclear spindle (tubulin staining coincident with the DAPI-stained nucleus) was calculated as the product of the pixel density and the area. The mean pixel density from randomly chosen cytoplasmic regions ($n > 15$) was multiplied by the mean area of the intranuclear spindles ($n > 100$) to obtain the intensity of background fluorescence. The mean background fluorescence was calculated and subtracted from the mean intranuclear fluorescence to obtain the corrected intensity of intranuclear fluorescence (± standard deviation). The relative fluorescence is expressed as a ratio of the corrected values (± standard deviation).

Karyogamy. Quantitative mating assays were performed by the method of Dutcher and Hartwell (14). Strains 404-4-12, 405-1-1, 5100-3-2, 5503-9-2, and BS213 were grown in YM-1 medium at 23°C to a cell density of 10^5/ml. *MAT***a** strains were arrested with α-factor for sufficient time to obtain 70 to 75% unbudded cells. α-Factor was removed by filtration, and the cells were resuspended in fresh YM-1 medium at a cell density of 10^6/ml; 2×10^6 cells from each parent of the opposite mating type were mixed and filtered onto 0.22-μm-pore-size GS Millipore filters (Millipore Corp., New Bedford, Mass.). The filters were placed onto YEPD plates and incubated at 28°C (maximal permissive temperature) for two generations' time. For matings involving wild-type and *kar1* strains, the filters were incubated for 4 h (28°C); for matings involving *cdc20* strains, the filters were incubated for 24 h at 28°C. The cells were washed from the filters in YM-1, sonicated, diluted, and plated at 23°C onto YEPD plates to determine the total number of viable cells and on SC medium lacking appropriate amino acids to select for prototrophic diploids. Cytoductants were selected on YEPG medium containing cycloheximide (10 μg/ml). Only cells that had completed cytoplasmic mixing but not nuclear fusion were cycloheximide resistant and respiratory competent and hence could form colonies on this medium. The percentage of input haploids that were cytoductants was calculated, and the ratio of cytoductants to diploids obtained in each mating was a measure of nuclear fusion (karyogamy) (14).

Nuclear migration. Strains 440-1-1 (*cdc20*) and 4958-3-2 (*CDC20*) were grown in liquid YM-1 medium at 23°C. Nocodazole was added to a final concentration of 15 μg/ml for 2.5 h at 23°C, and then cultures were shifted to 36°C for 20 min to inactivate Cdc20p in the presence of nocodazole. Cells were washed free of nocodazole with water preequilibrated at 36°C and resuspended in YM-1 at 36°C. Aliquots were taken every 15 min and fixed in 3.7% formaldehyde. Cells were stained with DAPI. Nuclear positions and morphologies were observed on a Zeiss Axiophot microscope equipped for epifluorescence. Quantitative analysis of nuclear position was done after the DAPI-stained cells were photographed on Kodak T-Max 400 films, and the negatives were developed as described above. The negatives were projected, and the positions of the nuclei were determined. The ratio of the shortest distance from the bud neck to any point on the nucleus and the maximum length of the mother cells as measured from the bud neck is defined as the nuclear migration index for that cell (28). The nuclear migration index was not calculated for unbudded cells or for cells in which the nuclei had already divided.

Analysis of tubulin levels. Strains 405-1-1 (*cdc20-1*) and 700-3-3 (*CDC20*) were grown to 2×10^7 cells per ml in YM-1 medium at 23°C, shifted to 36°C for 4 h, and then collected by centrifugation. Cells were disrupted by vortexing with glass beads in 20% trichloroacetic acid for 15 min. The beads were allowed to settle and were washed two times with 5% trichloroacetic acid, and the supernatants were pooled. Proteins were pelleted by centrifugation for 10 min at 4°C. The protein pellets were washed twice with acetone containing 0.9 M NH_4OH (−20°C). Protein samples were boiled after resuspension of the acid-insoluble pellets in sodium dodecyl sulfate-containing sample buffer as described by Laemmli (38). The protein concentration in the samples was determined by the Bradford protein assay as instructed by the manufacturer (Bio-Rad). The proteins were separated by polyacrylamide gel electrophoresis (PAGE) as described by Laemmli (38) and then transferred to nitrocellulose filters (20). The filters were incubated with rabbit polyclonal anti α-tubulin (anti-Tub1) antibody 345 (56) and stained with gold-conjugated goat anti-rabbit immunoglobulin G (Janssen Lifesciences Products Inc.). The gold-labelled antibody was detected according to the manufacturer's instructions.

DNA analysis and gap repair. The *CDC20* gene was cloned by *kar1*-mediated plasmid transfer (37), using strain GN46 as a donor and strain DK5201-4-3 as a recipient. A library of yeast genomic DNA fragments (*Sau*3A partial digests), cloned into a *CEN4 ARS1 LEU2* plasmid, was obtained from P. Hieter and transformed into the donor strain, GN46. The donors were mated to recipient strain DK5201-4-3, and the mated cells were replica plated to 36°C. Exceptional cytoductants were selected and tested for plasmid dependence by screening for plasmid loss after growth in YM-1 at 23°C and determining whether the strains that lost the plasmid also lost the complementing activity. Plasmid DNA (pDK362), recovered from one of the exceptional cytoductants, complemented the temperature sensitivity of *cdc20* strains upon retransformation.

Most DNA manipulations were done as described previously (54). Tn*5* mutagenesis was done as described elsewhere (11). Gapped plasmids were generated by digestion with restriction enzymes. The required DNA fragments were purified by agarose gel electrophoresis followed by electroelution of the DNA. An aliquot of the gapped plasmids was transformed into *Escherichia coli* DH5-α [F^- ϕ80d *lacZ* ΔM15 Δ(*lacZYA-argF*)*U169 recA1 endA1 hsdR17*(r_K^- m_K^+) *supE44 thi-1 gyrA relA1*] (Bethesda Research Laboratories) and plated onto solid medium containing ampicillin (50 μg/ml). No transformants were obtained on plates that had cells transformed with the gapped plasmids, confirming that all of the molecules were completely digested. DNA from this reaction was used to transform yeast strain 406-2-1 (*cdc20-1*) by the lithium acetate method. Transformants were selected on SC medium lacking leucine at 23°C and then replica plated at 36°C to determine the proportion of temperature-sensitive colonies. All of 80 colonies recovered after transformation with *Xba*I-gapped plasmids were temperature sensitive. All 10 of the repaired plasmids recovered from transformants were full length, which shows that the plasmids were repaired by gene conversion from chromosomal sequences and not by plasmid ligation. The tempera-

ture-sensitive mutation had been repaired onto the plasmid. To confirm that the *CDC20* gene was contained in pDK362, we integrated plasmid pMCM23 containing a 0.7-kb *Eco*RI-*Bam*HI fragment of the putative *CDC20* DNA cloned into plasmid YIp352 (24). The plasmid was digested with the restriction enzyme *Hpa*I, which cuts plasmid pMCM23 once within the *Eco*RI-*Bam*HI fragment. The linear DNA was transformed into the diploid strain 461, and approximately one-half of the transformants (101 of 233) were temperature sensitive. The temperature-sensitive transformants sporulated very poorly (<0.1%), and the spore viability was low (22%). We dissected 60 tetrads, and only 16 produced two viable spores; 21 produced only one viable spore, and there were no viable spores in the remaining 23 tetrads. All of the spores were temperature sensitive (*cdc20*), and none were *URA3*. These data show that the plasmid marker (*URA3*) was integrated into the *CDC20* allele in strain 461 and that the *CDC20* gene is essential for viability.

DNA sequencing. A 5.5-kb *Sac*I fragment from pDK362 was subcloned into pEMBL18, and nested deletions were prepared by using the Erase-a-Base system (Promega). Exonuclease III deletions were initiated after digesting the polylinker DNA with the enzymes *Sma*I and *Sal*I. The *Sal*I site was filled with α-phosphorothioate deoxynucleotides, and deletions were initiated from the *Sma*I site. Clones were selected that included the *CDC20* sequences (as determined by Tn*5* mapping), and double-stranded DNA was used for sequencing using the Sequenase system (U.S. Biochemical) and the M13 universal primer (Bethesda Research Laboratories) according to the manufacturer's instructions. One DNA strand was sequenced from the nested deletions and contained most of the *CDC20* open reading frame. The portion of the *CDC20* open reading frame that extended beyond the *Sac*I site was determined by preparing specific oligonucleotides (Operon Technologies) based on the sequence near the *Sac*I site. The predicted DNA sequence from the first strand was used to construct specific oligonucleotides (Operon Technologies) to prime sequencing reactions on the opposite strand. Both DNA strands encoding the *CDC20* gene were sequenced completely. The DNA sequences were assembled by using a Macintosh II personal computer and the DNA Inspector II software. The protein sequence was compared with sequences in the GenBank data base (1), using the FASTA program (39). Statistical significance of similarities was determined with the RDF algorithm by comparing an input sequence to random shuffles of the target sequence. The *Z* value was calculated as (similarity score − mean of the random scores/standard deviation of random scores).

Nucleotide sequence accession number. The sequence of the *CDC20* gene has been assigned EMBL accession number X59428 S. CEREVISIAE, CDC20 GENE.

RESULTS

Microtubule structure is altered in *cdc20* mutants. Hartwell and Smith (23) showed that chromosome losses are stimulated in *cdc20* mutants grown at a semipermissive temperature, suggesting that wild-type Cdc20p is required for chromosome segregation during mitosis. The effect of *cdc20* mutations on chromosome segregation could be explained if Cdc20p is required for assembly or function of the mitotic spindle. To determine whether *cdc20* affected microtubule structure, we observed the organization of microtubules in *cdc20* mutants by indirect immunofluorescence using an antitubulin antibody. Strain 405-1-1 (*cdc20*) was grown at the permissive temperature (23°C) to a cell density of 10^6/ml, and a sample was removed for analysis. The culture was shifted to the restrictive temperature (36°C), and samples taken at 5-min intervals were examined by immunofluorescence (Fig. 1). The mutant arrested with the terminal *cdc20* phenotype had intensely staining microtubule structures (Fig. 1D) compared with the same strain grown at the permissive temperature (Fig. 1A). The aberrant staining was evident in 70% of the cells (n = 200) at all stages of the cell cycle after incubation for 5 min at 36°C (Fig. 1b), and the staining was anomalous in over 95% of the cells (n = 200) by 20 min (Fig. 1c). Wild-type (*CDC20*) strain 700-3-3 showed no effect of short incubations at 36°C (not shown). We quantified the increase in tubulin staining in *cdc20* mutants by digital-enhanced microscopy by measuring the difference in the amount of fluorescence due to intranuclear staining in 100 cells from each of two strains, 405-1-1 (*cdc20*) and 700-3-3 (*CDC20*). We analyzed cells from strain 405-1-1 (*cdc20*) that were grown at 23°C or maintained at 36°C as described above. The cells from strain 700-3-3 (*CDC20*) were grown at 36°C, and cells that were budded with a single nucleus and a short spindle, and were therefore at the same approximate stage in the cell cycle as the *cdc20*-arrested cells, were analyzed. There was a fivefold increase (5.2 ± 1.7) in the relative fluorescence in the nuclei of cells from strain 405-1-1 (*cdc20*) (arrested for 4 h) compared with the nuclei in cells from the same strain grown at 23°C and a sevenfold increase (7.3 ± 2.3) compared with nuclei in wild-type cells.

To confirm that the aberrant microtubule staining in *cdc20* mutants resulted from a loss of *CDC20* function, we selected three temperature-resistant revertants that did not segregate the temperature sensitivity in meiosis (30 tetrads) and were thus considered intragenic. We examined the tubulin staining in each revertant after growth for 4 h at 36°C. The microtubule structure in revertants was indistinguishable from the microtubule structure in wild-type cells (data not shown). We conclude that the temperature sensitivity and the aberrant tubulin staining in strains carrying the *cdc20-1* mutation are both due to the loss of *CDC20* function.

The *CDC20* gene functions in G_1 mating cells. When an asynchronous population of *cdc20* cells was shifted from the permissive to the restrictive temperature, cells showed aberrant staining regardless of their morphology and hence position in the cell cycle (Fig. 1B and C). This finding suggests that the *CDC20* gene functions at multiple stages in the cell cycle. To extend this observation, we determined whether *cdc20* mutants had altered microtubule arrays at the mating step. Strains 4958-3-2 (*MAT***a** *bar1 CDC20*) and 440-1-1 (*MAT***a** *bar1 cdc20*) were grown at 23°C, and cells were arrested in the G_1 phase of the cell cycle by adding the mating pheromone α-factor. The arrested cells were shifted to the restrictive temperature in the presence of α-factor, incubated for 4 h, and then prepared for immunofluorescence using the antitubulin antibody. *cdc20* mutants arrested with α-factor stain more intensely with the antitubulin antibody (Fig. 2B) than do wild-type cells (Fig. 2A). These data suggest that the *CDC20* gene functions during mating.

We could determine whether the altered antitubulin staining pattern that we detected in α-factor-arrested *cdc20* mutants was correlated with abnormal microtubule function because microtubules are required for nuclear fusion during mating (12, 28, 40, 51). There is a simple genetic assay for karyogamy, and hence microtubule function, that detects cytoplasmic mixing in the absence of nuclear fusion (14). The assay utilizes two strains of opposite mating type, one having functional mitochondria ([*rho*$^+$]) and the other devoid

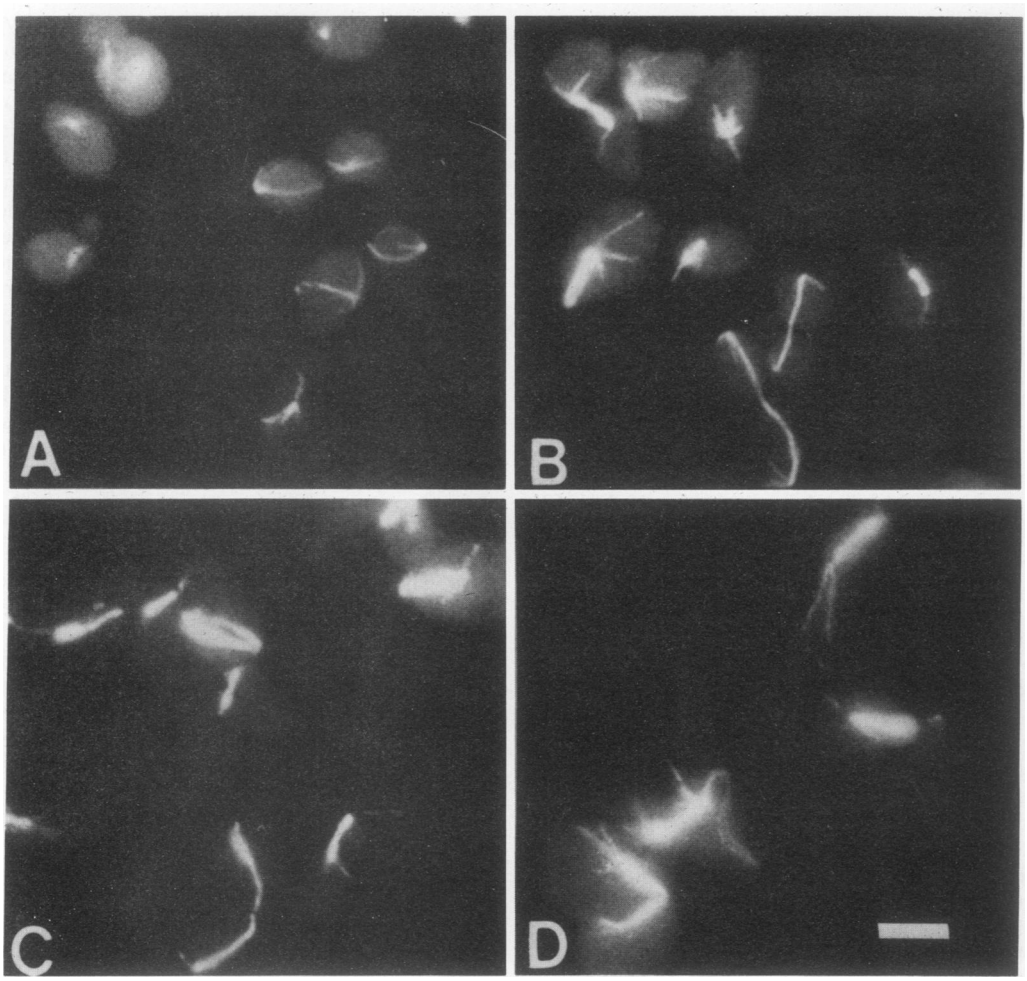

FIG. 1. Immunofluorescent tubulin staining in *cdc20* mutants. Strain 405-1-1 (*cdc20*) was grown to 10^6 cells per ml at 23°C and then incubated for various times at 36°C. (A) 23°C; (B) 36°C, 5 min; (C) 36°C, 20 min; (D) 36°C, 4 h.

of mitochondrial DNA ([*rho*^{0}]) but carrying a recessive nuclear mutation that confers drug resistance. Cells are mixed, allowed to mate, and then plated onto medium that selects for the drug-resistant (haploid) nucleus and functional mitochondria. The colonies that grow under these conditions derive from cells that have exchanged cytoplasmic contents of the parents but failed to complete nuclear fusion. We constructed appropriate strains and compared the efficiency of nuclear fusion after growth at 28°C, the maximal permissive temperature for the *cdc20-1* mutation. We used the maximal permissive temperature (the maximum temperature at which the mutants would divide) because the cells were limited in *CDC20* function, and we expected them to be compromised for microtubule function to the greatest extent. The results (Table 2) show that the ratio of cytoductants to diploids is increased 40-fold in *cdc20* × *cdc20* matings, indicating failures in nuclear fusion.

Nuclear migration is unaffected in *cdc20* mutants. *cdc20* mutations are pleiotropic, affecting three of the four known microtubule-mediated events (23, 47). *cdc20* mutants arrest in the cell cycle as budded cells with a single nucleus located at the neck. Therefore, at least one microtubule-dependent

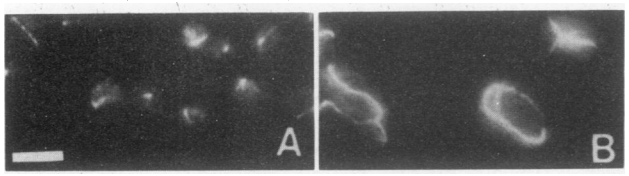

FIG. 2. Antitubulin staining in α-factor-arrested cells. Strain 4958-3-2 (*MAT***a** *bar1 CDC20*) (A) and strain 404-4-1 (*MAT***a** *bar1 cdc20*) (B) were arrested with α-factor and then incubated at 36°C before staining with antitubulin antibody YOL 1/34 as described in Materials and Methods.

TABLE 2. Karyogamy at 28°C

Crosses[a]	Mating efficiency (%)	% Cytoductants ([*rho*$^+$] *cyh*^{r})	Cytoductants/diploids[b]
WT × WT (5503-9-2 × 5100-3-2)	41.0	0.4	0.004
cdc20 × *cdc20* (405-1-1 × 404-4-12)	7.6	1.75	0.16
WT × *cdc20* (5503-9-2 × 404-4-12)	38.0	<0.01	<0.05
kar1 × WT (BS213 × 5100-3-2)	2.5	13.8	4.5
kar1 × *cdc20* (BS213 × 404-4-12)	0.5	18.0	7.0

[a] All strains are described in Materials and Methods. WT, wild-type (*CDC20 KAR1*) strain.

[b] Ratios of at least 2,000 diploids scored.

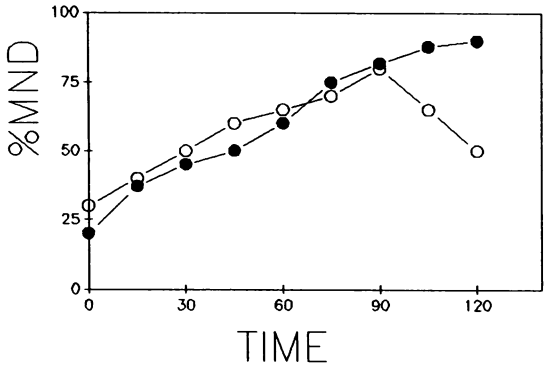

FIG. 3. Nuclear migration after nocodazole treatment. Strains 4958-3-2 (*CDC20*) and 440-1-1 (*cdc20*) were treated with nocodazole at 23°C to arrest the cells; the nocodazole was then washed away, and the cells were incubated at 36°C for the indicated times (minutes). Cells were then stained with DAPI and analyzed as described in Materials and Methods. Cells with nuclear migration indices between 0 and 0.2 had the single DAPI-staining nucleus at the neck and were considered as medial nuclear division (MND). Closed circles, strain 440-1-1; open circles, strain 4958-3-2.

event, nuclear migration, can occur in *cdc20* mutants. However, it is possible that the rate of nuclear migration is greatly impaired in *cdc20* mutants and that the 4-h incubation used to obtain the terminal *cdc* phenotype provides sufficient time to complete nuclear migration. It is difficult to measure the rate of nuclear migration during cell division in an asynchronous population of dividing cells. However, treating cells with nocodazole causes microtubules to depolymerize, and nuclei become randomly positioned within the cell (31). The microtubules quickly re-form when the drug is removed, and the nucleus migrates to the neck. We measured the kinetics of nuclear migration after nocodazole treatment to determine whether the rate was impaired in *cdc20* mutants. We treated strain 440-1-1 (*cdc20*) and strain 4958-3-2 (*CDC20*) with nocodazole at 23°C to arrest the cells with a nucleus that was randomly positioned in the cytoplasm. The cells were then shifted to the restrictive temperature for 20 min to inactivate Cdc20p in the presence of nocodazole. We infer from the data in Fig. 1 that Cdc20p was quickly inactivated and that the majority of cells were affected by 20 min. The cells were washed free of nocodazole while being maintained at 36°C, and the positions of the nuclei in the cells were determined by photographing DAPI-stained cells. The nuclei are considered to be properly positioned at the neck when the nuclear migration indices (see Materials and Methods) are between 0 and 0.2. The data (Fig. 3) show that nuclear migration proceeded at the same rate in *cdc20* mutants and wild-type cells, suggesting that there was a negligible effect of *cdc20* on nuclear migration.

The level of tubulin proteins is unaltered in *cdc20* mutants. Some of the pleiotropic phenotypes of *cdc20* mutants are similar to the phenotypes that result from overexpressing tubulin proteins (4, 32, 70). If *CDC20* regulated tubulin synthesis or accumulation, then the level of tubulin proteins should increase in *cdc20* mutants after incubation at 36°C. We compared the amounts of tubulin in strain 700-3-3 (*CDC20*) and strain 405-1-1 (*cdc20*) after growing cells at 36°C for 4 h and extracting protein. The total proteins from 10^7 cells and from serial twofold dilutions were separated by electrophoresis and transferred to nitrocellulose, and α-tubulin was detected with an anti-α-tubulin antibody. The

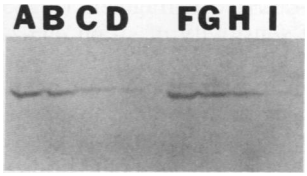

FIG. 4. Tubulin levels in *cdc20* mutants after incubation at 36°C. Strains 700-3-3 (*CDC20*) (lanes A to D) and 405-1-1 (*cdc20*) (lanes F to I) were incubated at 36°C for 4 h, and proteins were extracted as described in Materials and Methods. The proteins from 10^7 cells (lanes A and F) and from serial twofold dilutions (lanes B to D and G to I) were separated by PAGE, and α-tubulin was detected with antibody 345.

results (Fig. 4) show that there is a less than twofold increase in the amount of α-tubulin in *cdc20* mutants compared with wild-type cells. Similar results were obtained with an anti β-tubulin antibody probe (not shown). The small increase in tubulin protein in *cdc20* mutants is consistent with the twofold increase in the volume of mutant cells incubated at the restrictive temperature and is insufficient to account for the sevenfold increase in tubulin staining detected by quantitative immunofluorescence. We infer that the concentration of tubulin remains constant in the *cdc20* mutant and that the mutations affect tubulin assembly and not tubulin synthesis or accumulation.

***CDC20* is located on chromosome VII.** We cloned the DNA sequence that encodes the *CDC20* gene to facilitate mapping and to begin a molecular analysis of *CDC20* function. The gene was cloned by complementing the temperature sensitivity of a *cdc20* mutant as described in Materials and Methods. One plasmid, pDK362, was isolated, a partial restriction map was determined, and we showed that the plasmid encoded the *CDC20* gene by standard methods of gap repair (46) and plasmid integration as described in Materials and Methods and illustrated in Fig. 5.

To map the *CDC20* sequences within the 17 kb of genomic yeast DNA in plasmid pDK362, we mutagenized the plasmid with the bacterial transposon Tn*5*. Three Tn*5* insertions that mapped within a 2.0-kb region of the plasmid and eliminated *CDC20* function are shown in Fig. 5. The two Tn*5* insertions that did not eliminate the *cdc20*-complementing activity but defined the maximum extent of the *CDC20* gene are also

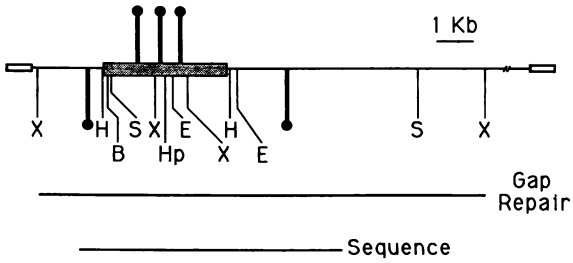

FIG. 5. Partial restriction map of plasmid pDK362. Shown are yeast genomic DNA (thin line), yeast shuttle vector (open box), and *CDC20* open reading frame (stippled box). Tn*5* insertions that eliminate *CDC20* function are above the line; Tn*5* insertions that have no effect on *CDC20* function are below the line. The DNA that was sequenced and the interval used in gap repair are indicated at the bottom. Only the portion of the yeast genomic DNA that contains *CDC20* is shown; the omitted sequences are indicated by a break in the DNA. Sites for restriction enzymes: B, *Bam*HI; E, *Eco*RI; H, *Hin*dIII; Hp, *Hpa*I; S, *Sac*I; X, *Xba*I.

shown. The 2.0-kb *Hin*dIII fragment (Fig. 5) complemented the temperature sensitivity of strain 406-2-1 after transformation when subcloned into YCp50.

We purified a 1.7-kb *Eco*RI fragment of DNA from pDK362 to use as a hybridization probe to localize the *CDC20* gene to chromosomal DNA separated by gel electrophoresis. We detected one band of hybridization (not shown) that contained two chromosomes, unresolved by electrophoresis, suggesting that *CDC20* was located on either chromosome VII or chromosome XV. We mapped *cdc20* to the left arm of chromosome VII by a three-factor cross involving *met13*, *cyh2*, and *cdc20*. The tetrad data showed parental ditype/nonparental ditype/tetratype ratios of 40/0/8 for *met13-cdc20*, 38/0/8 for *cyh2-cdc20*, and 25/0/15 for *met13-cyh2*. These data show that *cdc20* is between *met13* and *cyh2*, 8 centimorgans from *met13* and 10 centimorgans from *cyh2*. The *cyh2-met13* distance of 19 centimorgans is in agreement with published data (42). One other gene defined by the temperature-sensitive mutation, *tsm137*, has been mapped to this region (42). We tested whether *tsm137* was allelic to *cdc20* by standard complementation tests. *tsm137* complements the temperature sensitivity of *cdc20*, and therefore the two mutations are nonallelic. No other mutations that define essential genes or genes required for microtubule function have been mapped to the left arm of chromosome VII in the vicinity of *CDC20*.

Cdc20p shares homology with the β subunit of transducin. We sequenced a 2.64-kb region of the DNA including the sequences that complement the *cdc20-1* mutation. Analysis of the sequence showed a single large open reading frame encoding a protein with 519 amino acids and a predicted molecular size of 57.4 kDa. The complete sequences of the gene and the associated polypeptide are shown in Fig. 6. We sequenced two of the Tn*5* insertions that eliminated the activity of *CDC20*, and both insertions were within the open reading frame (not shown).

We compared the sequence of Cdc20p with sequences in the GenBank data base. Approximately half of the protein, the N-terminal 215 amino acids, showed no homology to other proteins. However, the computer identified homology in the C terminus of Cdc20p with several members of a family of proteins related to the regulatory (β) subunit of transducin, including human and bovine β-transducins, *S. cerevisiae MSI1* and *STE4* proteins, and the *Drosophila melanogaster E(spl)* gene product. Cdc20p shows at least 20% identity over at least 300 amino acids for each β-transducin homolog. The RDF algorithm of Lipman and Pearson (39) was used to evaluate the statistical significance of the comparison. The *Z* value (see Materials and Methods) was 17.2 standard deviations from the mean for Msilp and 9.9 standard deviations for both human β subunits, indicating significant similarity between Cdc20p and the other proteins. *CDC20*, like *MSI1* and *STE4*, is a member of a family of genes encoding β-transducin homologs in *S. cerevisiae* that also includes *CDC4*, *PRP4*, *TUP1*, and *MAK11* (10, 16, 29, 53, 71, 72). These proteins have a variable number of imperfect 43-amino-acid repeats that characterize mammalian β-transducins. Each repeat has a consensus sequence, but comparison of all of the members of the β-transducin family shows that there is variability at consensus sites. Furthermore, it is possible to align the repeats relative to the bovine sequence (16). Comparison of *CDC20* gene product with some members of the β-transducin family and the consensus sequence are shown in Fig. 7A. Alignment of the five β-transducin repeats in several of the members of the family is shown in Fig. 7B. Both the *CDC4* and *STE4* gene

```
                                                    M  P  E  S  S  R
-32          TATCAAAAGAGCAAGTATTACAAAGAAGACTAATGCCAGAAAGCTCTAGA
          D  K  G  N  A  A  I  S  G  N  R  S  V  L  S  I  A  S  P  T
18   GATAAGGGAAATGCAGCAATTAGCGGTAACCGTTCTGTACTTTCTATTGCGTCCCCAACA
          K  L  N  I  L  S  S  D  W  S  R  N  Q  G  K  V  S  K  N  S
78   AAGCTAAACATACTATCTTCCGATTGGTCCAGAAACCAAGGTAAAGTTTCTAAAAATTCG
          L  K  R  S  S  S  L  N  I  R  N  S  K  R  P  S  L  Q  A  S
138  CTAAAGAGATCAAGTTCACTGAACATTAGAAACTCCAAACGTCCCAGTTTACAAGCCTCT
          A  N  S  I  Y  S  R  P  K  I  T  I  G  A  P  P  L  I  R  R
199  GCCAATTCTATTTATTCAAGACCTAAGATTACAATTGGGGCACCACCGTTAATAAGACGA
          D  S  S  F  F  K  D  E  F  D  A  K  K  D  K  A  T  F  S  A
259  GATTCTTCATTTTTCAAAGATGAATTTGACGCTAAAAAAGACAAAGCAACGTTTTCGGCA
          V  S  S  R  S  Y  P  T  I  G  S  E  S  V  V  S  Q  T  S  L
319  TACTCTTCTCGTTCATATCCAACAATTGGATCTGAGAGCGTAGTTTCCCAAACATCTTTA
          S  Q  P  T  T  S  R  E  V  D  E  Q  F  T  V  A  A  D  R  Y
379  TCGCAACCGACAACATCTAGAGAAGTTGATGAGCAATTTACAGTAGCTGCGGATAGATAT
          I  P  I  L  Q  G  A  S  Q  N  K  V  D  P  E  T  L  H  E  A
409  ATTCCAATTCTACAGGGAGCTTCGCAAAACAAGGTCGATCCTGAAACCTTACACGAGGCA
          L  P  P  P  N  A  S  P  I  S  H  L  R  A  Q  T  K  I  V  F
469  TTACCTCCGCCAAACGCGTCGCCAATTTCACACTTAAGGGCCCAGACTAAGATTGTCTTC
          K  Q  N  V  A  E  A  C  G  L  D  M  N  K  R  I  L  Q  Y  M
529  AAACAAAATGTAGCTGAAGCGTGTGGGTTAGATATGAATAAAAGAATACTACAATACATG
          P  E  P  P  K  C  S  S  L  R  Q  K  S  Q  I  M  K  K  R  T
589  CCGGAACCACCAAAATGCTCTTCCTTGAGACAAAAAAGCTATATCATGAAGAAAAGAACA
          H  Y  S  Y  Q  Q  E  Q  K  I  P  D  L  I  K  L  R  K  I  N
649  CATTATAGTTATCAGCAGGAACAAAAAATTCCTGATTTAATTAAATTAAGGAAAATCAAT
          T  N  P  E  R  I  L  D  A  P  G  F  Q  D  D  F  Y  L  N  L
709  ACCAATCCGGAAAGAATTCTTGATGCACCTGGTTTCCAAGACGACTTTTATTTAAACTTG
          L  S  W  S  K  K  N  V  L  A  I  A  L  D  T  A  L  Y  L  W
769  TTAAGTTGGTCCAAAAAAAAATGTCTTAGCTATAGCACTAGACACTGCATTATATCTGTGG
          N  A  T  T  G  D  V  S  L  L  T  D  F  E  N  T  T  I  C  S
829  AATGCCACCACTGGGGATGTTTCCCTGTTAACGGATTTCGAAAACACCACAATATGCAGC
          V  T  W  S  D  D  D  C  H  I  S  M  A  K  E  D  G  N  T  E
889  GTTACGTGGTCTGATGATGATTGTCATATCTCTATGGCTAAAGAGGATGGGAACACCGAA
          I  W  D  V  E  T  M  S  L  I  R  T  M  R  S  G  L  G  V  R
949  ATTTGGGACGTTGAGACCATGTCATTAATTAGAACTATGAGATCAGGCTTAGGTGTCCGT
          I  G  S  L  S  W  L  D  T  L  I  A  T  G  S  R  S  G  E  I
1009 ATCGGTTCATTGTCTTGGTTAGATACTTTGATAGCTACAGGCAGTCGTAGTGGAGAAATT
          Q  I  N  D  V  R  I  K  Q  H  I  V  S  T  W  A  E  H  T  G
1069 CAAATCAATGATGTCAGGATCAAACAGCATATTGTATCTACATGGGCAGAGCACACAGGC
          E  V  C  G  L  S  Y  K  S  D  G  L  Q  L  A  S  G  G  N  D
1129 GAAGTCTGCGGTTTGAGCTATAAAAGTGACGGATTGCAACTTGCATCTGGTGGTAATGAT
          N  T  V  M  I  W  D  T  R  T  S  L  P  Q  F  S  K  K  T  H
1189 AACACTGTAATGATTTGGGATACCAGAACGTCCTTGCCTCAATTTTCCAAGAAGACGCAT
          T  A  A  V  K  A  L  S  W  C  P  Y  S  P  N  I  L  A  S  G
1249 ACTGCTGCTGTAAAAGCACTAAGCTGGTGTCCATATTCGCCAAATATTCTAGCCTCTGGA
          G  G  Q  T  D  K  H  I  H  F  W  N  S  I  T  G  A  R  V  G
1309 GGCGGACAAACAGATAAACACATCCATTTTTGGAACAGTATCACAGGTGCACGAGTTGGC
          S  I  N  T  G  S  Q  V  S  S  L  H  W  G  Q  S  H  T  S  T
1369 TCAATCAATACCGGATCCCAGGTGAGCTCTTTACATTGGGGCCAAAGTCATACGTCAACC
          N  G  G  M  M  N  K  E  I  V  A  T  G  G  N  Q  R  M  Q  S
1429 AATGGTGGTATGATGAATAAAGAGATTGTTGCCACAGGAGGTAATCAGAGAATGCAATCT
          L  F  I  I  M  K  Q  N  S  K  L  Q  K  *
1489 CTGTTTATAATTATGAAACAAAATTCAAAGTTGCAGAAGTAGTTCATGCTCATGAAGCAA
```

FIG. 6. DNA sequence of the *CDC20* gene and the predicted protein sequence. The nucleotide sequence is numbered beginning at the A of the initiator ATG.

products have all eight of the repeats. The *MSI1* protein has an extra repeat, and both the *PRP4* and *CDC20* proteins have five repeats that align differently with respect to the bovine sequence.

DISCUSSION

We have shown that the microtubule staining pattern, assayed by indirect immunofluorescence using an antitubulin antibody, is anomalous in *cdc20* mutants. The aberrant staining pattern of microtubules is due to the *cdc20-1* mutation because the temperature-sensitive growth and the unusual staining pattern in *cdc20* mutants can be reverted in a single step. The DNA fragment that complements the temperature-sensitive growth defect also suppresses the antitubulin staining phenotype in the mutants (5). The anomalous tubulin staining phenotype is not restricted to strains with the *cdc20-1* allele, reported here, but is also detectable in strains with two other *cdc20* alleles (62). Our data suggest that altered microtubule assembly is the primary defect in *cdc20* mutants, although it is possible that the *CDC20* gene affects microtubule assembly indirectly. For example, the

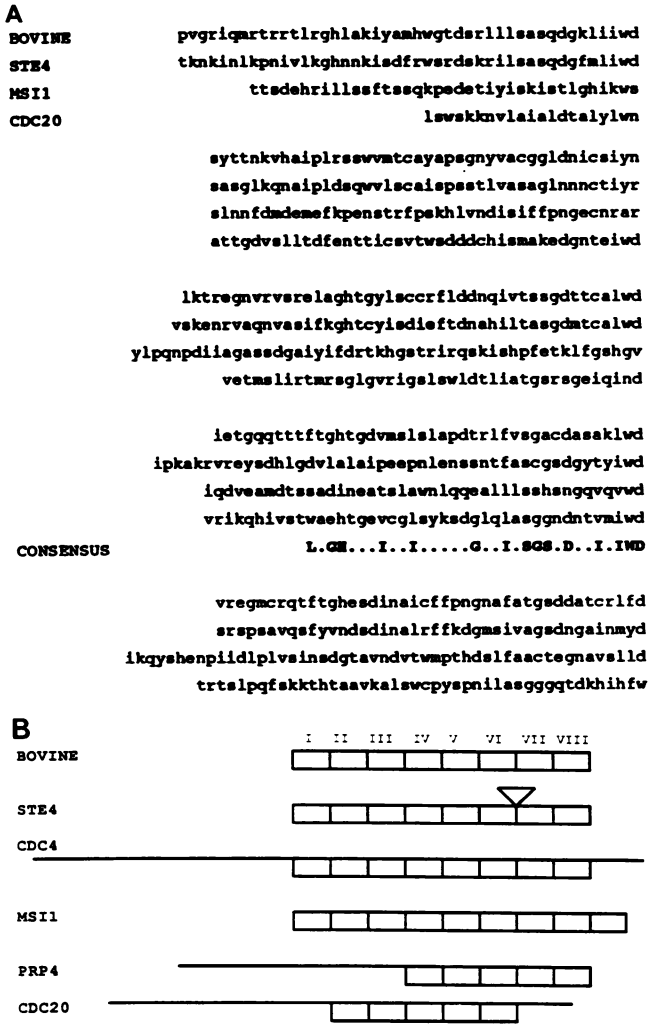

FIG. 7. Alignment of Cdc20p with other members of the β-transducin family, using FASTA. (A) Alignment of the Cdc20p sequence, beginning at amino acid 267, the bovine β-transducin sequence, and sequences of the products of two other yeast genes that encode β-transducin homologs, *STE4* and *MSI1*. The alignments were provided by FASTA. The blocks of amino acids correspond to the five β-transducin repeats that are present in Cdc20p. The consensus sequence is for the β-transducin repeat shown under the fourth repeat. (B) Individual β-transducin repeats of the bovine sequence, numbered I to VIII. Sequences of various members of the β-transducin family from *S. cerevisiae* are aligned with the bovine sequence relative to the numbered repeats. The straight lines in the sequences for the *CDC4*, *PRP4*, and *CDC20* gene products represent N-terminal sequences that are unrelated to β-transducin. The *STE4* protein has a sequence unrelated to β-transducin that separated repeats VI and VII.

aberrant microtubule structures in *cdc20* mutants may be the indirect consequence of the physiological state of the arrested cells. Although we cannot rule out this possibility, we think it unlikely because other *cdc* mutants that arrest with the same terminal phenotype as *cdc20* do not show aberrant tubulin staining (62). The pleiotropy of *cdc20* mutants is similar to that of *tub* mutants (28, 58), which suggests that *CDC20* is involved directly in microtubule assembly and that the multiple phenotypes of *cdc20* mutants are explainable in terms of failures in microtubule function.

Two previous observations also suggest a role for *CDC20* in microtubule-mediated events. *CDC20* is required for mitotic chromosome segregation (23) and nuclear transits (47), the microtubule-dependent movements of nuclei between the mother and daughter cell prior to mitosis. We have extended the previous observations to demonstrate a role for *CDC20* in karyogamy. Dutcher and Hartwell (14) analyzed a large collection of *cdc* mutants for effects on karyogamy in an attempt to identify genes required for nuclear fusion during mating. The assay was designed to detect those genes, like *KAR1*, with unilateral karyogamy defects (only one parent being mutant). We also observed no effect on the efficiency of karyogamy when we performed a similar mating, but we could detect a bilateral effect on karyogamy (both parents were mutant). We infer that the wild-type Cdc20p is not nuclear limited and can mix prior to functioning in *cdc20* × wild-type matings. There are several other bilateral karyogamy mutations that behave like *cdc20* (26, 28, 40, 51, 58). Many of the mutations, such as *tub1*, *tub2*, *kar1*, *kar3*, *cin1*, *cin2*, and *cin4*, are also pleiotropic like *cdc20*, and the primary defect is in microtubule function.

The phenotypes of *cdc20* mutants are also similar to the phenotypes described when α- and β-tubulin are overproduced (4, 70). Elaborate microtubule staining is observed, microtubule-dependent events such as chromosome segregation and karyogamy are affected, and cells become inviable. Quantitative analysis of the increased antitubulin staining in *cdc20* mutants showed a sevenfold increase in the amount of tubulin staining in the intranuclear spindles, yet quantitative Western immunoblots showed that the tubulin levels increased by less than a factor of 2. It is possible *CDC20* affects tubulin synthesis and that there is a slight increase in the concentration of tubulin in the mutants that exceeds the critical concentration for assembly, resulting in the excessive microtubule staining. Although we cannot rule out this possibility, we think it unlikely because the anomalous tubulin staining associated with *cdc20* mutants is induced quickly and because *S. cerevisiae* cells are relatively insensitive to alterations (decreases) in tubulin concentration (32). We favor the model that *CDC20* affects microtubule structure or assembly.

One simple model that explains the anomalous microtubule staining is that *cdc20* mutants have the normal amount of tubulin assembled into a dysfunctional polymer and that some property of the microtubules in the mutant results in exposing a larger number of the tubulin epitopes to the antibodies. We dislike this model for several reasons. We have used two antibodies in addition to YOL 1/34 to stain microtubules in *cdc20* mutants, and the anomalous staining is independent of the antibody used. The epitopes for all three of the tubulin antibodies are known. Antibodies 345 (anti-α-tubulin) and FY145 (anti-β-tubulin) are antipeptide antibodies to unique C-terminal peptides of both proteins (2, 56). The acidic C-terminal domains of the tubulins are exposed on the face in the microtubule polymer and are thought to facilitate interactions with microtubule-associated proteins (60). There is no unique epitope for the monoclonal anti-α-tubulin antibody YOL 1/34, suggesting that the antibody recognizes a conformation that extends over a large region of the protein (61). Therefore, exposing more tubulin epitopes to these three antibodies would mean that the entire surface of the microtubules is affected. A large number of tubulin epitopes on the surface of the microtubule might be exposed in *cdc20* mutants if Cdc20p were a microtubule-binding protein that normally blocks accessibility of the antibodies to the tubulin. Although we cannot rule out this

possibility, it seems unlikely for two reasons. First, Cdc20p would have to mask the majority of tubulin epitopes and would therefore have to be an abundant protein and a major constituent of yeast microtubule cytoskeleton. Current biochemical data suggest that there are microtubule-associated proteins in yeast cells but they are not abundant (33, 49). Second, there are no consensus tubulin-binding domains, defined by other microtubule-associated proteins (25, 44) identifiable in the sequence of Cdc20p.

Another possible model that explains the anomalous tubulin staining in *cdc20* mutants is that the wild-type *CDC20* product is required for microtubule disassembly. If the increased fluorescence that we measured in *cdc20* mutants is due to excess tubulin dimers assembled into polymer, then the majority of tubulin in wild-type cells must be in the unassembled pool. Our estimates of the amount of tubulin that is assembled into the mitotic spindle are consistent with this model. Peterson and Ris (48) showed that haploid yeast cells with a fully formed spindle (medial nuclear division) contain, at most, 20 microtubules per half spindle with an average length of 0.25 μm and 5 pole-to-pole microtubules with a maximum length of 1.25 μm. Assuming that there are 1,500 tubulin dimers per μm of microtubule (13), the medial nuclear division spindle of a yeast cell should contain 4.4×10^{-15} g of tubulin. Tubulin represents 0.7% of the total cell protein (19), and a haploid yeast cell contains 6×10^{-12} g of protein (63); therefore, there is approximately 4.2×10^{-14} g of tubulin per cell. Therefore, 10% of the total cellular tubulin is normally assembled into the intranuclear spindle prior to anaphase. These estimates are consistent with the model that the function of *CDC20* is to promote microtubule disassembly.

Cdc20p functions at more than one step in the life cycle, since three microtubule-dependent events, karyogamy, nuclear transits, and chromosome segregation (mitosis), are affected. One microtubule-mediated event, nuclear migration, is unaffected in the *cdc20* mutant. There are two simple models that could explain these observations. One possibility is that Cdc20p functions only when it is required. Alternatively, Cdc20p may function continuously but some microtubule-mediated events may not require microtubule disassembly. If the three microtubule-dependent events, karyogamy, nuclear transits, and chromosome segregation, require microtubule disassembly, each would be affected in *cdc20* mutants. If nuclear migration requires only microtubule assembly, it could be unaffected in the *cdc20* mutant.

The analysis of the protein-coding sequence of the cloned DNA suggests that Cdc20p has two domains, one of which shares some homology with the β subunit of transducin. The amino acid identity is low (20%), but the sequence homology extends over a large region of the protein, 300 amino acids, and is statistically significant (39). In addition to the amino acid homology, there are five contiguous repeated motifs common to members of the β-transducin family (15) that are present in Cdc20p. Other members of the β-transducin family in *S. cerevisiae* include the products of *CDC4*, *MAK11*, *MSI1*, *PRP4*, *TUP1*, and *STE4* (10, 16, 29, 53, 71). Identifying the β-transducin repeats provides a molecular framework for thinking about *CDC20* function. Many β-transducins function in GTP-dependent signal transduction pathways (17), and it is possible that Cdc20p, like Ste4p, is involved in some intracellular signalling event. Cdc20p could possibly play a more direct role in microtubule assembly by somehow modulating GTP binding to tubulin. Unfortunately, there is no known function for the repeated motifs in the mammalian β-transducin or any of the members of the β-transducin family (10). One recent report suggests that the repeats facilitate protein-protein interactions because Tup1p physically interacts with Cyc8p to form a complex (73). Cyc8p is also a member of a family of proteins that have a tetratricopeptide (TPR) repeat (18), and the TPR family includes two other *CDC* genes, *CDC16* and *CDC23*. We are currently testing for genetic interactions of these *CDC* genes and for physical interactions among their products.

ACKNOWLEDGMENTS

We thank Lee Hartwell, Bob Sclafani, Phil Hieter, and the Yeast Genetic Stock Center for providing strains and plasmids. We thank Lenny Rebhun and Mark Neff for critical comments on the manuscript.

This work was supported by a March of Dimes Birth Defects Foundation Basil O'Connor Scholarship and by National Institutes of Health grant GM 40334-02 to D.J.B. D.K. is a Lucille P. Markey Scholar; this work was supported in part by the Lucille P. Markey Charitable Trust.

REFERENCES

1. **Bilofsky, H. S., D. Burks, J. W. Fickett, W. B. Goad, F. I. Lewitter, W. P. Rindone, C. D. Swindell, and C. S. Tung.** 1986. The GenBank genetic sequence database. Gene **14**:1–4.
2. **Bond, J. F., J. L. Fridovich-Keil, L. Pillus, R. C. Mulligan, and F. Solomon.** 1986. A chicken-yeast chimeric beta-tubulin protein is incorporated into mouse microtubules in vivo. Cell **44**:461–468.
3. **Botstein, D., N. Segev, T. Stearns, M. A. Hoyt, J. Holden, and R. A. Kahn.** 1988. Diverse biological functions of small GTP-binding proteins in yeast. Cold Spring Harbor Symp. Quant. Biol. **53**:629–636.
4. **Burke, D., P. Gasdaska, and L. Hartwell.** 1989. Dominant effects of tubulin overexpression in *Saccharomyces cerevisiae*. Mol. Cell. Biol. **9**:1049–159.
5. **Burke, D. J.** Unpublished observations.
6. **Byers, B.** 1981. Cytology of the yeast life cycle, p. 59–96. *In* J. N. Strathern, E. W. Jones, and J. R. Broach (ed.), The molecular biology of the yeast *Saccharomyces*: life cycle and inheritance. Cold Spring Harbor Laboratory, Cold Spring Harbor, N.Y.
7. **Byers, B., and L. Goetsch.** 1974. Duplication of spindle plaques and integration of the yeast cell cycle. Cold Spring Harbor Symp. Quant. Biol. **38**:123–131.
8. **Byers, B., and L. Goetsch.** 1975. Behavior of spindles and spindle plaques in the cell cycle and conjugation of *Saccharomyces cerevisiae*. J. Bacteriol. **124**:511–523.
9. **Conde, J., and G. R. Fink.** 1976. A mutant of *Saccharomyces cerevisiae* defective in nuclear fusion. Proc. Natl. Acad. Sci. USA **73**:3651–3655.
10. **Dalrymple, M. A., S. Petersen-Bjorn, J. D. Friesen, and J. D. Beggs.** 1989. The product of the *PRP4* gene of *S. cerevisiae* shows homology to the beta subunits of G proteins. Cell **58**:511–512.
11. **de Bruijn, F. J., and J. R. Lupski.** 1984. The use of transposon Tn5 in the rapid generation of correlated genetic and physical maps of DNA segments cloned into multicopy plasmids—a review. Gene **27**:131–149.
12. **Delgado, M. A., and J. Conde.** 1984. Benomyl prevents nuclear fusion in *Saccharomyces cerevisiae*. Mol. Gen. Genet. **193**:188–189.
13. **Dustin, P.** 1984. Microtubules. Springer-Verlag, New York.
14. **Dutcher, S. K., and L. H. Hartwell.** 1982. The role of *S. cerevisiae* cell division cycle genes in nuclear fusion. Genetics **100**:175–84.
15. **Fong, H. K. W., T. T. Amatruda, B. W. Birren, and M. I. Simon.** 1987. Distinct forms of the B subunit of GTP-binding regulatory proteins identified by molecular cloning. Proc. Natl. Acad. Sci. USA **84**:3792–3796.
16. **Fong, H. K. W., J. B. Hurley, R. S. Hopkins, R. Miake-Lye, M. Johnson, R. Doolittle, and M. I. Simon.** 1986. Repetitive seg-

mental structure of the transducin beta subunit: homology with the *CDC4* gene and identification of related mRNA's. Proc. Natl. Acad. Sci. USA **83**:2162–2166.
17. **Gilman, A.** 1987. G proteins: transducers of receptor generated signals. Annu. Rev. Biochem. **56**:615–649.
18. **Goebl, M., and M. Yanagida.** 1991. The TPR snap helix: a novel protein repeat motif from mitosis to transcription. Trends Biochem. Sci. **16**:173–177.
19. **Gullov, K., and J. Friis.** 1980. Chromosomal proteins in *Saccharomyces cerevisiae*. Curr. Genet. **2**:69–74.
20. **Harlow, E., and D. Lane.** 1988. Antibodies: a laboratory manual. Cold Spring Harbor Laboratory, Cold Spring Harbor, N.Y.
21. **Hartwell, L. H.** 1967. Macromolecular synthesis in temperature-sensitive mutants of yeast. J. Bacteriol. **93**:1662–1670.
22. **Hartwell, L. H., R. K. Mortimer, J. Culotti, and M. Culotti.** 1973. Genetic control of the cell division cycle in yeast. V. Genetic analysis of *cdc* mutants. Genetics **74**:267–286.
23. **Hartwell, L. H., and D. Smith.** 1985. Altered fidelity of mitotic chromosome transmission in cell cycle mutants of *S. cerevisiae*. Genetics **110**:381–395.
24. **Hill, J. E., A. M. Myers, T. J. Koerner, and A. Tzagoloff.** 1986. Yeast/*E. coli* shuttle vectors with multiple unique restriction sites. Yeast **2**:163–167.
25. **Himmler, A., D. Drechsel, M. W. Kirschner, and D. W. Martin, Jr.** 1989. Tau consists of a set of proteins with repeated C-terminal microtubule-binding domains and variable N-terminal domains. Mol. Cell. Biol. **9**:1381–1388.
26. **Hoyt, M. A., T. Stearns, and D. Botstein.** 1990. Chromosome instability mutants of *Saccharomyces cerevisiae* that are defective in microtubule-mediated processes. Mol. Cell. Biol. **10**:223–234.
27. **Huffaker, T. C., M. A. Hoyt, and D. Botstein.** 1987. Genetic analysis of the yeast cytoskeleton. Annu. Rev. Genet. **21**:259–284.
28. **Huffaker, T. C., J. H. Thomas, and D. Botstein.** 1988. Diverse effects of beta-tubulin mutations on microtubule formation and function. J. Cell Biol. **106**:1997–2010.
29. **Icho, T., and R. B. Wickner.** 1988. The *MAK11* protein is essential for cell growth and replication of double-stranded RNA and is apparently a membrane-associated protein. J. Biol. Chem. **263**:1467–1475.
30. **Ito, H., Y. Fukada, K. Murata, and A. Kimura.** 1983. Transformation of intact yeast with alkali cations. J. Bacteriol. **153**:163–168.
31. **Jacobs, C. W., A. E. Adams, P. J. Szaniszlo, and J. R. Pringle.** 1988. Functions of microtubules in the *Saccharomyces cerevisiae* cell cycle. J. Cell Biol. **107**:1409–1426.
32. **Katz, W., B. Weinstein, and F. Solomon.** 1990. Regulation of tubulin levels and microtubule assembly in *Saccharomyces cerevisiae*: consequences of altered tubulin gene copy number. Mol. Cell. Biol. **10**:5286–5294.
33. **Kilmartin, J. V.** 1981. Purification of yeast tubulin by self-assembly. Biochemistry **20**:3629–3633.
34. **Kilmartin, J. V., and A. E. Adams.** 1984. Structural rearrangements of tubulin and actin during the cell cycle of the yeast *Saccharomyces*. J. Cell Biol. **98**:922–933.
35. **Kirschner, M., and T. Mitchison.** 1986. Beyond self-assembly: from microtubules to morphogenesis. Cell **45**:329–342.
36. **Kirschner, M. W.** 1987. Biological implications of microtubule dynamics. Harvey Lect. **83**:1–20.
37. **Koshland, D., J. C. Kent, and L. H. Hartwell.** 1985. Genetic analysis of the mitotic transmission of minichromosomes. Cell **40**:393–403.
38. **Laemmli, U. K.** 1970. Cleavage of structural proteins during the assembly of the head of bacteriophage T4. Nature (London) **227**:680–685.
39. **Lipman, D. J., and W. R. Pearson.** 1985. Rapid and sensitive protein similarity searches. Science **227**:1435–1441.
40. **Meluh, P. B., and M. D. Rose.** 1990. *KAR3*, a kinesin-related gene required for yeast nuclear fusion. Cell **60**:1029–1041. (Erratum, **61**:548.)
41. **Mitchison, T., and M. Kirschner.** 1984. Dynamic instability of microtubule growth. Nature (London) **312**:237–242.
42. **Mortimer, R. K., D. Schild, C. R. Contopoulou, and J. A. Kans.** 1989. Genetic map of *Saccharomyces cerevisiae*, edition 10. Yeast **5**:321–403.
43. **Neff, N. F., J. H. Thomas, P. Grisafi, and D. Botstein.** 1983. Isolation of the beta-tubulin gene from yeast and demonstration of its essential function in vivo. Cell **33**:211–219.
44. **Noble, M., S. A. Lewis, and N. J. Cowan.** 1989. The microtubule binding domain of the microtubule-associated protein MAP1B contains a repeated motif unrelated to MAP2 and TAU. J. Cell Biol. **109**:3367–3376.
45. **Olmstead, J. B.** 1986. Microtubule-associated proteins. Annu. Rev. Cell Biol. **2**:421–457.
46. **Orr-Weaver, T., J. Szostak, and R. Rothstein.** 1983. Genetic applications of transformation with linear and gapped plasmids. Methods Enzymol. **101**:228–245.
47. **Palmer, R. E., M. Koval, and D. Koshland.** 1989. The dynamics of chromosome movement in the budding yeast *Saccharomyces cerevisiae*. J. Cell Biol. **109**:3355–3366.
48. **Peterson, J. B., and H. Ris.** 1976. Electron-microscopic study of the spindle and chromosome movement in the yeast *Saccharomyces cerevisiae*. J. Cell Sci. **22**:219–242.
49. **Pillus, L., and F. Solomon.** 1986. Components of microtubular structures in *Saccharomyces cerevisiae*. Proc. Natl. Acad. Sci. USA **83**:2468–2472.
50. **Pringle, J. R., and L. H. Hartwell.** 1981. The *Saccharomyces cerevisiae* cell cycle, p. 97–142. *In* J. N. Strathern, E. W. Jones, and J. R. Broach (ed.), The molecular biology of the yeast *Saccharomyces*: life cycle and inheritance. Cold Spring Harbor Laboratory, Cold Spring Harbor, N.Y.
51. **Rose, M. D., and G. R. Fink.** 1987. *KAR1*, a gene required for function of both intranuclear and extranuclear microtubules in yeast. Cell **48**:1047–1060.
52. **Rose, M. D., P. Novick, J. H. Thomas, D. Botstein, and G. R. Fink.** 1987. A *Saccharomyces cerevisiae* genomic plasmid bank based on a centromere-containing shuttle vector. Gene **60**:237–243.
53. **Ruggieri, R., K. Tanaka, M. Nakafuku, Y. Kaziro, A. Toh-e, and K. Matsumoto.** 1989. MSI1, a negative regulator of the RAS-cAMP pathway in *Saccharomyces cerevisiae*. Proc. Natl. Acad. Sci. USA **86**:8778–8782.
54. **Sambrook, J., E. F. Fritsch, and T. Maniatis.** 1989. Molecular cloning: a laboratory manual. Cold Spring Harbor Laboratory, Cold Spring Harbor, N.Y.
55. **Sammak, P. J., G. J. Gorbsky, and G. G. Borisy.** 1987. Microtubule dynamics in vivo: a test of mechanisms of turnover. J. Cell Biol. **104**:395–405.
56. **Schatz, P. J., G. E. Georges, F. Solomon, and D. Botstein.** 1987. Insertions of up to 17 amino acids into a region of alpha-tubulin do not disrupt function in vivo. Mol. Cell. Biol. **7**:3799–3805.
57. **Schatz, P. J., L. Pillus, P. Grisafi, F. Solomon, and D. Botstein.** 1986. Two functional alpha-tubulin genes of the yeast *Saccharomyces cerevisiae* encode divergent proteins. Mol. Cell. Biol. **6**:3711–3721.
58. **Schatz, P. J., F. Solomon, and D. Botstein.** 1988. Isolation and characterization of conditional-lethal mutations in the TUB1 alpha-tubulin gene of the yeast *Saccharomyces cerevisiae*. Genetics **120**:681–695.
59. **Schulze, E., and M. Kirschner.** 1987. Dynamic and stable populations of microtubules in cells. J. Cell Biol. **104**:277–288.
60. **Serrano, L., J. de la Torre, R. B. Maccioni, and J. Avila.** 1984. Involvement of the carboxy-terminal domain of tubulin in the regulation of its assembly. Proc. Natl. Acad. Sci. USA **81**:5989–5993.
61. **Serrano, L., F. Wandosell, and J. Avila.** 1986. Location of the regions recognized by five commercial antibodies on the tubulin molecule. Anal. Biochem. **159**:253–259.
62. **Sethi, N.** Unpublished observations.
63. **Sherman, F.** 1991. Getting started with yeast, p. 3–21. *In* C. Guthrie and G. R. Fink (ed.), Guide to yeast genetics and molecular biology. Academic Press, New York.
64. **Sherman, F., G. R. Fink, and J. B. Hicks.** 1986. Laboratory course manual for methods in yeast genetics. Cold Spring Harbor Laboratory, Cold Spring Harbor, N.Y.

65. **Shero, J., M. Koval, F. Spencer, R. E. Palmer, P. Hieter, and D. Koshland.** 1991. Analysis of chromosome segregation in *Saccharomyces cerevisiae*, p. 749–773. *In* C. Guthrie and G. R. Fink (ed.), Guide to yeast genetics and molecular biology. Academic Press, New York.
66. **Spencer, F., S. L. Gerring, C. Connelly, and P. Hieter.** 1990. Mitotic chromosome transmission fidelity mutants in *Saccharomyces cerevisiae*. Genetics **124**:237–249.
67. **Stearns, T., and D. Botstein.** 1988. Unlinked noncomplementation: isolation of new conditional-lethal mutations in each of the tubulin genes of *Saccharomyces cerevisiae*. Genetics **119**:249–260.
68. **Stearns, T., M. A. Hoyt, and D. Botstein.** 1990. Yeast mutants sensitive to antimicrotubule drugs define three genes that affect microtubule function. Genetics **124**:251–262.
69. **Thomas, J. H., N. F. Neff, and D. Botstein.** 1985. Isolation and characterization of mutations in the beta-tubulin gene of *Saccharomyces cerevisiae*. Genetics **111**:715–734.
70. **Weinstein, B., and F. Solomon.** 1990. Phenotypic consequences of tubulin overproduction in *Saccharomyces cerevisiae*: differences between alpha-tubulin and beta-tubulin. Mol. Cell. Biol. **10**:5295–5304.
71. **Whiteway, M., L. Hougan, D. Dignard, D. Y. Thomas, L. Bell, G. C. Saari, F. J. Grant, P. O'Hara, and V. L. MacKay.** 1989. The *STE4* and *STE18* genes of yeast encode potential beta and gamma subunits of the mating factor receptor-coupled G protein. Cell **56**:467–477.
72. **Williams, F. E., and R. J. Trumbly.** 1990. Characterization of *TUP1*, a mediator of glucose repression in *Saccharomyces cerevisiae*. Mol. Cell. Biol. **10**:6500–6511.
73. **Williams, F. E., U. Varanasi, and R. J. Trumbly.** 1991. The CYC8 and TUP1 proteins involved in glucose repression in *Saccharomyces cerevisiae* are associated in a protein complex. Mol. Cell. Biol. **11**:3307–3316.
74. **Williamson, D. H., and D. J. Fennell.** 1975. The use of fluorescent DNA binding agent for detecting and separating yeast mitochondrial DNA. Methods Cell Biol. **12**:335–351.
75. **Yochem, J., and B. Byers.** 1987. Structural comparison of the yeast cell division cycle gene *CDC4* and a related pseudogene. J. Mol. Biol. **195**:233–245.